

## Symmetry Energy in the Inner Crust Region of Neutron Stars: A Study Around the Neutron Drip Density Point using the Compressed Liquid Drop Model

Eko Tri Sulistyani✉, Yusuf Panji Wisnuaji, Romy Hanang Setya Budhi  
Department of Physics, FMIPA, Universitas Gadjah Mada, Yogyakarta, Indonesia

### Article Info

Article history:  
Submitted 5 June 2023  
Revised 27 August 2023  
Accepted 28 August 2023

Keywords:  
symmetry energy, neutron drip,  
inner crust, compressible liquid  
drop model

### Abstract

The properties of neutron star's inner crust have been investigated using the Compressible Liquid Drop Model, particularly around the neutron drip density region, which is the boundary between the outer and inner crust. Symmetry energy in the equations of state SLy4 and BSk3 was calculated to determine the density data between the outer and inner crusts. The properties of the inner crust can be understood through parameters such as the change in the number of nucleons in the atomic nucleus, the asymmetry parameter in surface energy, and volume energy. It was shown that the choice of the symmetry energy expansion coefficient ( $L$ ) of order-1 results in a distinct energy range of 9-11 MeV within the neutron drip region. This contrasts significantly with the energy symmetry observed around saturation density, which reaches  $(30 \pm 4)$  MeV in the reference models used. Furthermore, it was found that symmetry energy affects the neutron composition in the inner crust. As the density increases, neutron numbers rise, while proton counts exhibit relative stability within the range of 40 to 50 for each atomic nucleus. Importantly, we observe a marked decrease in proton fraction at the onset of the neutron drip region, where  $E_{sym} \cong 10$  MeV, suggesting electron capture processes transforming protons into neutrons. This phenomenon contributes to the presence of neutron and free neutron gas layers within the inner crust.

## INTRODUCTION

Stars are massive balls of luminous gas ( $M > 0,08M_{\odot}$ ) and are formed from molecular clouds (high-density interstellar gas and dust) that eventually clump together due to gravitational forces between the molecules (Istiqomah, 2010). Neutron

stars are objects of matter that are highly compressed in such a way that the geometry of space-time changes from flat space-time (Weber, 2005). The relativistic contribution to the hydrostatic equilibrium equation of stellar structure is expressed by the TOV (Tolman-Oppenheimer-Volkoff) equation (Misner *et al.*, 1973; Oppenheimer and Volkoff, 1939; Tolman, 1939) :

$$\frac{dP}{dr} = -G \frac{\rho m}{r^2} \left(1 - \frac{P}{\rho c^2}\right) \left(1 + \frac{4\pi P R^3}{m c^2}\right) \left(1 - \frac{2Gm}{rc^2}\right)^{-1} \quad (1)$$

$$\frac{dm}{dr} = 4\pi r^2 \rho \quad (2)$$

$$\frac{d\Phi}{dr} = -\frac{1}{\rho c^2} \frac{dP}{dr} \left(1 + \frac{P}{\rho c^2}\right)^{-1} \quad (3)$$

The equation above relates the pressure  $P(r)$ , density of the star  $\rho(r)$ , the mass of the star  $m(r)$  and the components of the metric tensor  $\Phi(r)$  (Haensel, P., Potekhin, A.Y., and Yakovlev, D.G., 2007). Solving the TOV equation requires knowledge of the relationship between pressure  $P(r)$ , star density  $\rho(r)$ , which is commonly referred to as the equation of states (*EoS*).  $P = P(\rho)$ . Knowledge of the *EoS* is required to calculate the properties of neutron stars, such as to determine the maximum mass of neutron stars ( $M_{max}$ ). Compact objects with masses greater than the maximum mass of a neutron star ( $M > M_{max}$ ), can certainly be identified as black holes (Douchin and Haensel, 2001).

The structure of a neutron star generally consists of an outer and inner core, an outer and inner crust, and an atmosphere, and there is a boundary layer between the outer core and the inner crust called the **mantle** or **paste phase**, and a boundary between the inner crust and the outer crust called the **neutron drip region**. It is called the neutron drip region because in this region neutrons begin to drip out of the core. It is not possible to know the structure and state of neutron stars directly. Observations made for neutron stars are only based on the emitted spectrum and the results obtained in the form of luminosity, spectrum energy (frequency and wavelength) can be used to determine the mass, radius, and surface temperature of neutron stars in general. However, the structure and state of matter in neutron stars cannot be known with certainty through observation.

The use of the compressed liquid drop model to determine the inner crust properties of neutron stars is based on the fact that the neutron density increases continuously towards the core of the neutron star. The core material in the neutron star's inner crust is viewed as clusters. The core clusters in the inner crust are modeled as liquid drops whose energy,  $E(A, Z)$  can be decomposed into volume

terms, surface terms and Coulomb terms as a function of density.

The compressed liquid drop model is a mass model built from the Weizsacker-Bethe mass formula by adding coefficients from volume effects, surface, and symmetry terms as a function of density. In general, the advantage of the compressed liquid drop model is that it can explain a wide variety of macroscopic properties of nuclei. Over the past decade, the model has been used to explain neutron skins, deformation of rapidly rotating nuclei, synthesis of superheavy nuclei, nuclear fission reactions, and nuclei in the inner crust of stars.

One of the main elements of *EoS* that has become of great interest in the field of astrophysics for dense neutron matter is the symmetry energy (Lee, *et al.*, 1998). This *EoS* is the bridge that connects the knowledge between symmetry energy and structure in neutron stars, such as the surface effect, Coulomb effect, and volume effect (Gandolfi, 2013). Symmetry energy appears when the system deviates from the isospin symmetric limit of an equal number of neutrons and protons. (Roca-Maza and Piekarewicz, 2008). The investigation of symmetry energies in neutron stars is increasingly vigorous. Starting from symmetry energy in general to symmetry energy on each structure contained in neutron stars has been studied in various methods, such as Thomas-Fermi calculations, Brueckner-Hartree-Fock approach with all kinds of variations, relativistic and non-relativistic and other approaches. In this study, the effect of symmetry energy on the properties of the neutron star crust was studied, especially in the neutron drop density region, which is the boundary between the outer and inner crusts, described by the compressible liquid drop model.

### Neutron Star

Neutron star with typical mass  $M = (1 \sim 2)M_{\odot}$ , with  $M_{\odot} = 2 \times 10^{33}$  g is the mass of the sun,

has a radius of  $R \approx (10 - 14)$  km. Density  $\rho$  of the star is  $\sim 10^{15}$  g cm<sup>-3</sup>, or approximately 3 times the density of a normal nucleus  $\rho_0 = 2,8 \times 10^{14}$  gcm<sup>-3</sup> (Potekhin, 2010). Neutron stars have minimum and maximum mass limits. The maximum mass lies in the range  $(1,44 \sim 3)M_{\odot}$  (Lattimer and Prakash, 2004).

Basically, the regions of neutron stars are divided into the core and the envelope. The envelope of a neutron star consists of the atmosphere, ocean layer, outer crust, inner crust, and mantle. The core of a neutron star consists of the inner core and outer core (Haensel *et al.*, 2007).

- Atmosphere: Neutron star atmospheres vary in depth from deep  $\sim 10$  cm for hot neutron stars and can disappear for cool neutron stars.
- Ocean Layer: The depth of the ocean layer of neutron stars  $\sim 10 - 100$  m, with mass density  $\rho \sim 10^6 - 10^9$  g cm<sup>-3</sup>.
- Outer crust: The depth of the outer crust is  $\sim 10 - 100$  m, with mass density  $10^6$  g cm<sup>-3</sup>  $\lesssim$
- $\rho \lesssim 4,3 \times 10^{11}$  g cm<sup>-3</sup>, and consists of a plasma of ions and electrons.

- Deep crust: Deep crust has a depth  $\sim 1 - 2$  km and its density  $\rho \approx (4 - 6) \times 10^{11}$  g cm<sup>-3</sup>. The material contained in the deep crust is electrons, free neutrons (neutron gas), atomic nuclei rich in neutrons.
- The outer core: The outer core of a neutron star has a depth of several kilometers and a density of  $0,5 \rho_0 \lesssim \rho \lesssim 2\rho_0$ . The material of the outer core is composition  $n\bar{p}e\mu$ .
- Inner core: The inner core of a star is dense  $\rho \gtrsim 2\rho_0$  and is several kilometers deep. The density of the inner core can even reach  $\rho \sim 10 - 15 \rho_0$

The crust is a component that plays an important role in the evolution of neutron stars (Pawel Haensel, 2001). At **Figure 1**, we can see the changes in the atomic nuclei of the neutron star structure in general. The nuclei change with each increase in density, from freely scattered nuclei to organized nuclei. Then the nuclei that have an excess of neutrons, leading to the fusion of each nucleus into a homogeneous core.

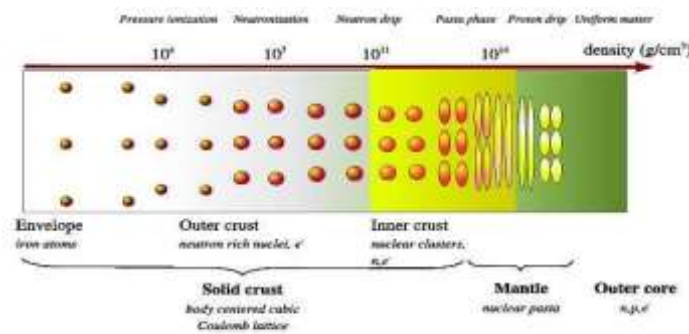


**Figure 1.** Schematic structure of the neutron star crust (Chamel and Haensel, 2008)

The region where the core begins to drip neutrons due to an excess of neutrons in the core is the boundary region between the outer crust and the inner crust. The area is referred to as the neutron drip region, which can be seen in **Figure 2**. As the

density increases, the ground state value  $Z/A$  decreases and neutrons become increasingly unbound.

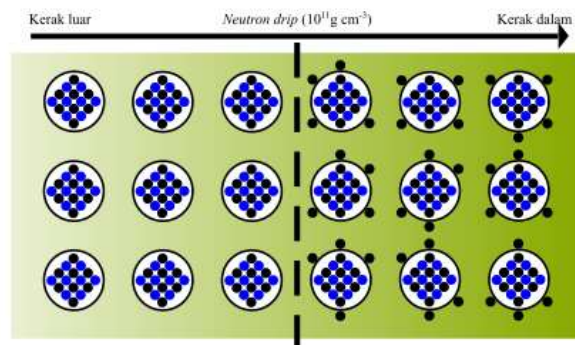


**Figure 2.** The transition region between the outer crust and the inner crust in neutron stars with neutrons (black dots) and protons (blue dots) in the core

If we define pure neutron chemical potential in a nucleus

$$\mu'_n \equiv \mu_n - m_n c^2 = \left( \frac{\partial E\{A,Z\}}{\partial N} \right)_Z - m_n c^2, \quad (4)$$

As long as  $\mu'_n < 0$ , all neutrons are bound inside the nucleus. The neutron drip region corresponds to  $\mu'_n = 0$ . Beyond this point, neutrons drip out of the nucleus, i.e. neutrons begin to populate states with the continuous energy spectrum. The neutron drip point can be roughly estimated using mass formula approximation  $E\{A, Z\} = E\{A, Z\} - Amc^2$ , where the neutron-proton mass difference is ignored,  $m_n \approx m_p \approx m = 939 \text{ MeV } c^{-2}$ . By neglecting the surface term and the Coulomb term, we get

$$E\{A, Z\} \approx A \left( E_{vol} + E_{sym} \delta^2 \right), \quad (5)$$

with  $\delta \equiv \frac{N-Z}{A}$ , and  $E_{vol}$  and  $E_{sym}$  are experimental volume energy and symmetry energy of the nucleus,  $E_{vol} \approx -16 \text{ MeV}$  and  $E_{sym} \approx 32 \text{ MeV}$  respectively. Using equation (5), it can be easily shown that the value of  $\delta$  with  $\mu'_n = 0$  is

$$\delta_{ND} = \sqrt{1 - E_{vol}/E_{sym}} - 1 \approx 0.225 \quad (6)$$

By neglected neutron-proton mass difference, the equilibrium condition of the  $\beta^-$

$$p + e \rightarrow n + \nu_e \quad (7)$$

with

$$\mu_e = \mu_n - \mu_p \approx 4E_{sym} \delta \quad (8)$$

Then the proton fraction can be written as follows (Haensel *et al.*, 2007)

$$x_p = Z/A \approx 4,75 \times 10^{-2} \left( \frac{\rho_0}{\rho} \right) \left( \frac{E_{sym}(\rho)}{E_{sym}(\rho_0)} \right)^3. \quad (9)$$

### Compressed Liquid Drop Model

The atomic nucleus is composed of nucleons so that interactions between nucleons can affect the density of the nucleus. The interactions between nucleons at the surface of the nucleus are different from those at the center of the nucleus. Therefore, a review of surface effects is essential for the nucleon

density. As the nucleon density increases, the pressure increases. This affects the density equilibrium of the compressed nucleon liquid. To see this effect, CLDM is used, which includes a Semi-Empirical Mass Formula that depends on the density of the nucleus given as the density of barions and excess neutrons in the interior of the nucleus. The matter density following the neutron droplets  $\rho_{ND}$  is not only relevant for the crusts of neutron stars, but also for white dwarfs (Chamel dan Haensel, 2008). The total energy density in the outer crustal layer is given as follows (Baym, Pethick *et al.*, 1971).

$$\varepsilon_{tot} = n_N E(A, Z) + \varepsilon_e + \varepsilon_L, \quad (10)$$

with  $n_N$  is the number density of nuclei,  $E(A, Z)$  is the energy of nuclei with  $Z$  is number of protons and  $A$  the number of nucleons in the atomic nucleus,  $\varepsilon_e$  is the kinetic energy density of electrons that arise due to interactions between electrons and between electrons and positive ion core clusters,  $\varepsilon_L$  is the lattice energy density that arises due to interactions between clusters.

Upon entering the deep crust, appear additional interactions due to excess neutrons/neutrons that are not bound to the nucleus, results in a decrease in surface tension along with an increase in density, and compression of matter inside the nucleus (Paweł Haensel, 2001), so that the total energy density in equation (10) gets a contribution from the free neutron gas  $\varepsilon_n$  (Chamel and Haensel, 2008)

$$\varepsilon_{tot} = n_N E(A, Z) + \varepsilon_e + \varepsilon_L + \varepsilon_n. \quad (11)$$

The binding energy of each nucleus is given as follows (Douchin and Haensel, 2001).

$$E(A, Z) = E_{vol} + E_{surf} + E_{Coul}. \quad (12)$$

Element  $E_{vol}$  is the volume energy with the bulk contribution of the nucleon, which is independent of the size and shape of the nucleus structure (Haensel, 2001; Iida and Oyamatsu, 2004).

$$E_{vol} = Aw(\rho, \delta), \quad (13)$$

with the bulk contribution of each nucleon being

$$w(\rho, \delta) = a_{vol} + \frac{K}{18} \left( \frac{\rho - \rho_0}{\rho_0} \right)^2 + \left[ J + \frac{L}{3} \left( \frac{\rho - \rho_0}{\rho_0} \right) \right] \delta^2, \quad (14)$$

here  $K$  is the incompressibility, while  $J$  is the volume symmetry coefficient and  $L$  is the density symmetry coefficient. The surface energy can be written (Oyamatsu *et al.*, 2010)

$$E_{surf} = 4\pi\sigma(\rho, \delta)r_p^2, \quad (15)$$

with surface potential  $\sigma$  as a function of density  $\rho$  and asymmetry parameter  $\delta$ :

$$\sigma(\rho, \delta) = \sigma_0 \left[ 1 - C_{sym}\delta^2 + \chi \left( \frac{\rho - \rho_0}{\rho_0} \right) \right], \quad (16)$$

with  $C_{sym}$  is the symmetry coefficient of surface energy. Surface potential per unit area  $\sigma$  and the chemical potential  $\mu_{n,s}$  of neutrons absorbed on the droplet surface, forming a neutron shell, can be determined by

$$\sigma = \frac{\partial E_{surf}}{\partial \mathcal{A}} \Big|_{N_s}, \quad \mu_{n,s} = \frac{\partial E_{surf}}{\partial N_s} \Big|_{\mathcal{A}}, \quad (17)$$

where  $\mathcal{A}$  ( $4\pi r_p^2$  for spherical nuclei) is the cell surface area, while  $N_s$  is the number of neutrons in the neutron shell. By using Euler's theorem approach on homogeneous functions, the surface energy can be written as (Chamel and Haensel, 2008)

$$E_{surf} = \sigma \mathcal{A} + N_s \mu_{n,s}. \quad (18)$$

With a simple approach, the curvature correction in  $E_{surf}$  is proportional to  $\mathcal{A}/r_p$  so it can be neglected, while  $\sigma$  can be approximated by the surface tension  $\sigma_{surf}$ , and  $N_s = v_{surf} \mathcal{A} \simeq (\rho_{n,i} - \rho_{n,o}) s_n \mathcal{A}$ , with

$$E(\rho, \delta) = E(\rho, \delta = 0) + E_{sym,2}(\rho)\delta^2 + E_{sym,4}(\rho)\delta^4 + \dots + E_{sym,2k}(\rho)\delta^{2k} + \dots, \quad (21)$$

with  $\rho = \rho_p + \rho_n$  is the total density, and  $\delta = 1 - 2x_p$  where  $x_p$  is the proton fraction (Gandolfi, 2013; Sammarruca, 2014).

Nuclear matter with equal numbers of neutrons and protons ( $x_p = 0.5$ ) is referred to as symmetric nuclear matter (SNM), and nuclear matter with  $x_p = 0.0$  is naturally referred to as pure neutron matter (PNM) (Newton *et al.*, 2012). Parameters  $E(\rho, \delta = 0)$  is the energy per baryon of core symmetry matter, while the expansion coefficient is (Moustakidis, 2012).

$v_{surf}$  is the surface density of absorbed neutrons (Haensel *et al.*, 2007).

The Coulomb energy derived for the radius of a uniformly charged sphere  $r_p$  is given by (Chamel dan Haensel, 2008)

$$E_{Coul} = \frac{3Z^2e^2}{5r_p}. \quad (19)$$

The relationship between surface energy and Coulomb energy can simply be written

$$E_{surf} = 2E_{Coul} \quad (20)$$

as a result of the virial theorem on simplified CLDM without curvature correction (Baym *et al.*, 1971).

### Symmetry Energy

Symmetry energy is the energy difference between pure neutron matter and symmetry core matter. The stability of the matter in neutron stars is sensitive to the existence of symmetry energy and its first derivatives. Neutrons cannot survive the saturation density, so they will turn into protons through decay of  $\beta^-$ . The cooling of neutron stars is strongly related to the fraction of protons and neutrons as a function of density. (Gandolfi, 2013). Symmetry energy appears in the equation of state of nuclear matter subject to Taylor expansion as a function of density and isospin asymmetry terms. The isospin asymmetry term ( $\delta$ ) describes the state of matter when the proton fraction is not equal to the neutron fraction. Energy per particle  $E(\rho, \delta)$  in basic asymmetric nuclear matter can be expanded around  $\delta = 0$  corresponding to symmetry matter so that it becomes as follows (Moustakidis, 2012).

$$\begin{aligned} E_{sym,2}(\rho) &= \frac{1}{2!} \frac{\partial^2 E(\rho, \delta)}{\partial \delta^2} \Big|_{\delta=0}, \\ E_{sym,4}(\rho) &= \frac{1}{4!} \frac{\partial^4 E(\rho, \delta)}{\partial \delta^4} \Big|_{\delta=0}, \\ E_{sym,2k}(\rho) &= \frac{1}{(2k)!} \frac{\partial^{2k} E(\rho, \delta)}{\partial \delta^{2k}} \Big|_{\delta=0}. \end{aligned} \quad (22)$$

Based on equation (21), only  $\delta$  even powers have a great influence because the strong interaction must be symmetrical between the number of neutrons and protons. The parameter  $E_{sym,2k}(\rho)$  is the multiplying coefficient of the isospin asymmetry term with an approximation of order more than 2 can be ignored because the value is too small, so in the case of an

expansion independent of the asymmetry parameter  $\delta$ , the symmetry energy can be defined as

$$E_{sym}(\rho) = E(\rho, \delta = 1) - E(\rho, \delta = 0), \quad (23)$$

and the energy per particle can be written

$$E(\rho, \delta) = E(\rho, \delta = 0) + (E(\rho, \delta = 1) - E(\rho, \delta = 0)) \delta^2. \quad (24)$$

The energy at saturation density is  $E(\rho_0) = -16$  MeV and its symmetry energy can be expanded as (Gandolfi, 2013; Baldo dan Burgio, 2016)

$$E_{sym}(\rho) = J + \frac{L}{3} \left( \frac{\rho - \rho_0}{\rho_0} \right) + \frac{K_{sym}}{18} \left( \frac{\rho - \rho_0}{\rho_0} \right)^2 + \frac{Q_{sym}}{162} \left( \frac{\rho - \rho_0}{\rho_0} \right)^3 + \dots, \quad (25)$$

with symmetry energy parameters, namely  $J$ ,  $L$ ,  $K_{sym}$  and  $Q_{sym}$ . Parameter  $J$  is the symmetry energy at saturation density

$$J = E_{sym}(\rho_0), \quad (26)$$

parameter  $L$  is the coefficient of the first-order expansion parameter in the expansion  $E_{sym}(\rho)$  around the saturated density which represents the slope of the symmetry energy graph with respect to density

$$L = 3\rho_0 \left( \frac{dE_{sym}}{d\rho} \right)_{\rho_0}, \quad (27)$$

while  $K_{sym}$  is the second-order expansion parameter that describes the curvature of the graph

$$K_{sym} = (3\rho_0)^2 \left( \frac{d^2 E_{sym}}{d\rho^2} \right)_{\rho_0}. \quad (28)$$

The form of the symmetry energy equation in equation (25) continues to higher powers ( $Q_{sym}$  and so on)

$$Q_{sym} = (3\rho_0)^3 \left( \frac{d^3 E_{sym}}{d\rho^3} \right)_{\rho_0}. \quad (29)$$

However, all parameters with rank  $> 2$  are ignored, leaving the parameters  $J$ ,  $L$ , dan  $K_{sym}$  (Newton *et al.*, 2012; Baldo and Burgio, 2016).

## RESULTS AND DISCUSSION

Calculation of symmetry energy against density based on equation (25) using several *EoS* models as examples, namely SLy4 as the main model and BSk3 as well as Z model, MSk9 model, and SkI5 according to (Danielewicz dan Lee, 2009) as comparison models. The results of the symmetry energy calculation are shown in **Figure 3**.

The calculation results shown in **Figure 3** are in line with the results of the calculation of symmetry energy as a function of density in (Paweł Danielewicz dan Lee, 2009). It can be seen in **Figure 3** that the increase in symmetry energy is consistent with the increase in density for all four models used. However, as the density approaches saturation density, there are some models that depict decreasing symmetry energy. This occurs as a result of the density symmetry coefficient which describes the slope of the symmetry energy graph.  $L$  which describes the slope of the symmetry energy graph.

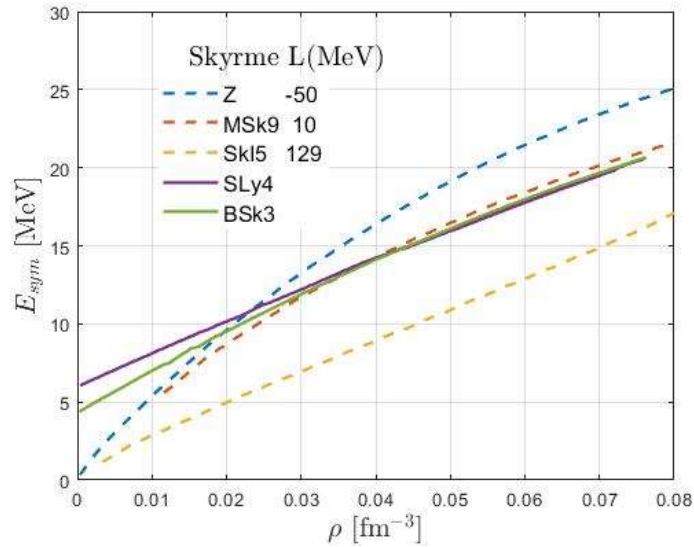


**Figure 3.** Symmetry energy as a function of density with several *EoS* models.

The symmetry energies in the neutron drop region only in the range of 9 MeV to 11 MeV for the SLy4, BSk3, and Z models are certainly very different from the symmetry energies around the saturation density which reach  $(30 \pm 4)$  MeV (Zhang dan Chen, 2013), while the value of the density symmetry coefficient  $L$  around neutron drops ( $\rho \approx 4 \times 10^{-3} \text{ fm}^{-3}$ ) for the three models used are still quite relevant, as seen from **Figure 3** where the value of symmetry energy increases in line with the increase

of density. However, in the saturation region,  $L$  in the Z model is no longer relevant because the value of  $L$  in model Z is not in the specified range, namely (20 ~ 115) MeV (Zhang dan Chen, 2013).

Symmetry energy affects the composition of the deep crust visualized in **Figure 4**. In the neutron drop region with  $E_{sym}$  range of (9 ~ 11) MeV, one can see the appearance of  $N_s$ . This is certainly related to the neutrons that begin to drip from the atomic nucleus.

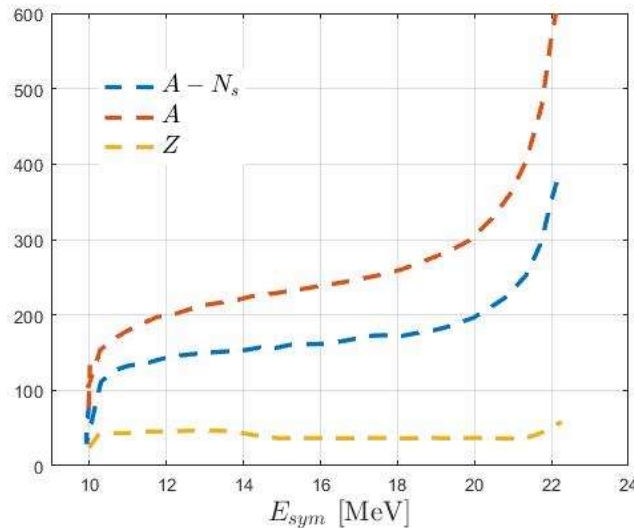


**Figure 4.** Change in deep crustal composition versus symmetry energy as a function of density

As the density increases, it can be seen that  $Z$  tends to stabilize between 40 and 50, but the number of  $A$  and  $N_s$  increases as it splits into two segments. At the time of  $E_{sym} = (11 \sim 19)$  MeV, the increase in the number of  $A$  and  $N_s$  is stable and tends to be gradual. Whereas at  $E_{sym} > 19$  MeV, the increase in the number of  $A$  and  $N_s$  is very high. However, the

increase in the number of neutrons that form the neutron shell  $N_s$  is decreasing. This occurs because as one goes deeper into the pasta-nucleus phase interface of the star, the atomic nuclei become more homogeneous.

**Figure 4** shows that the symmetry energy has a relationship with the proton fraction, which can

also be seen in Eq. (9). The dependence of symmetry energy on proton fraction as one of the compositions in the deep crust can also be observed in **Figure 5**. The proton fraction, besides depending on the number of  $Z$  and  $A$ , also has a relationship with  $E_{sym}$  with  $\rho$ , as seen in equation (9). A drastic decrease in proton fraction at the beginning of the neutron drop region with  $E_{sym} \cong 10$  MeV, occurs when  $N$  at stable numbers at 40, 50 and 82 to reduce the electronic contribution. The results shown in **Figure 5** are a small subset of those obtained by (Pearson *et al.*, 2014).

The decrease of  $x_p = Z/A$  occurs because degenerate electrons dominate and make protons

capture electrons so that equilibrium  $-\beta$  occurs as in equation (7). The proton fraction slopes and gets smaller towards 5% at the saturation density. However, at  $\rho \geq \rho_0$ , the process is reversed because the neutrons are unable to maintain the condition, so they decay and make the proton fraction  $x_p$  starts to increase. Thus, proton neutronization gives way to neutron protonization through  $\beta$  decay. However, the increase in the number of  $Z$  will not exceed the amount  $N$  in the nucleus of the neutron star.

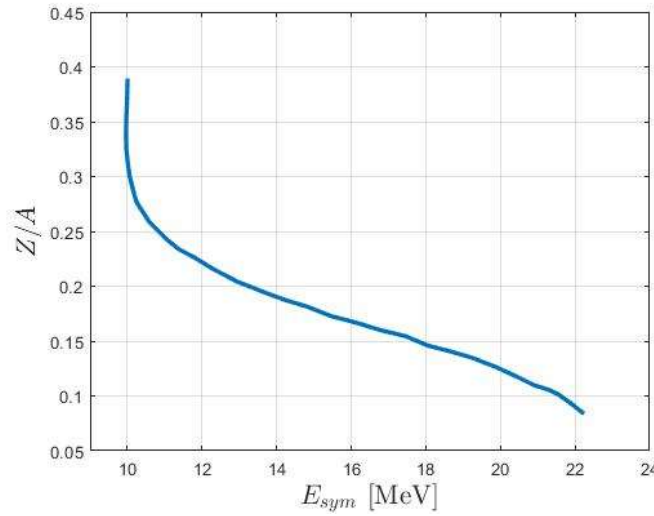


**Figure 5.** Dependence of proton fraction  $Z/A$  to the symmetry energy  $E_{sym}$ .

The correlation of symmetry energy to surface energy is connected through the local asymmetry parameter  $\delta_L$  which describes the number of adsorbed neutrons forming a neutron shell (Steiner *et al.*, 2005).

$$N_s = 4\pi r_p^2 \frac{C_{sym} \delta_L}{E_{sym}(1 - \delta_L)}, \quad (30)$$

with

$$\delta_L = \frac{A - N_s - 2Z}{A - N_s}. \quad (31)$$

From equation (31), then it can be written as

$$N_s = \frac{A(\delta - \delta_L)}{(1 - \delta_L)}, \quad (32)$$

with

$$\delta_L = \delta \left[ 1 + \frac{4\pi r_p^2 C_{sym}}{E_{sym} A} \right]^{-1}. \quad (33)$$

The local asymmetry parameter starts to appear when there are atoms with excess neutron and starting to form a neutron shell which starts to occur before the neutron drop region ( $\rho \leq 4 \times 10^{-3} \text{ fm}^{-3}$ ). The difference between  $\delta$  with  $\delta_L$  can be seen in **Figure 6**.



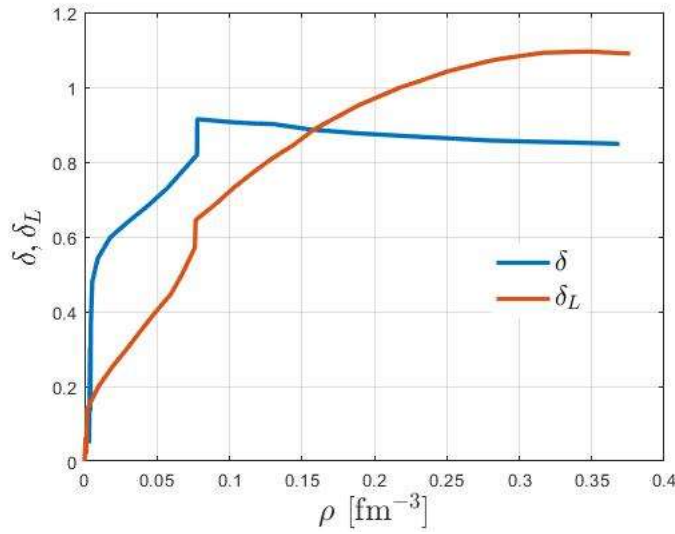


**Figure 6.** Local asymmetry parameters  $\delta_L$  and asymmetry parameters  $\delta$  in the paste phase region up to twice the saturation density in neutron star cores as a function of density

Equation (33) tell us that the difference in value between  $\delta_L$  with the value of  $\delta$  rise with the increase in the number of  $A$  and with the increase of neutron accumulation at the surface of the atomic nucleus represented by  $4\pi r_p^2 C_{sym}$ .

At the time of  $\rho \approx 0,08 \text{ fm}^{-3}$  a discontinuity occurs, which is caused by the changing shape of the atomic nucleus. This indicates that the region is beginning to enter the neutron star pasta phase. At  $\rho \approx 0,16 \text{ fm}^{-3}$ , value of  $\delta_L$  is equal to the value of  $\delta$  which indicates that its density is the saturation point of the neutron stars. In the region  $\rho_0$  up to  $2\rho_0$ , the value of  $\delta_L$  exceeds the value of  $\delta$  due to the start

of the fusion of each atomic nucleus towards homogeneous in the core region of the neutron star. The decrease in the value of  $\delta$  value, which is quite gentle, occurs due to the protonization of neutrons which makes the number of  $Z$  slightly increases, while the value of  $\delta_L$  continues to increase because the number of  $A$  and  $E_{sym}$  keep increasing.

Equation (33) is also the link between the symmetry energy and the local asymmetry parameter with the value of  $C_{sym} = 2$  (Iida and Oyamatsu, 2004) and can be shown through **Figure 7**.

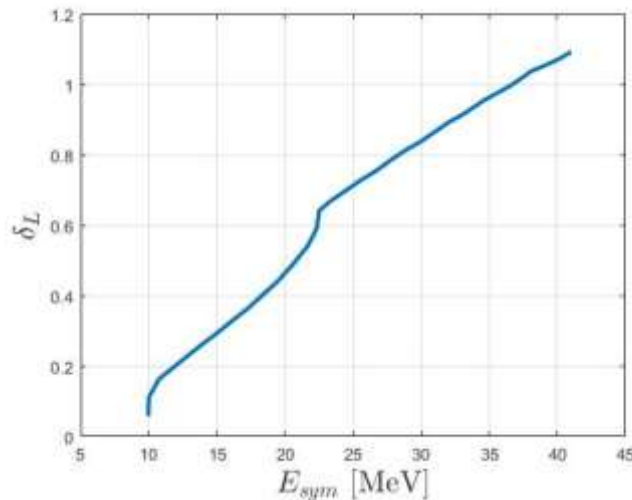


**Figure 7.** Relationship between local asymmetry parameter  $\delta_L$  with symmetry energy  $E_{sym}$

**Figure 7** is a graph of the correlation between the magnitude of the local asymmetry parameter and the symmetry energy, which is directly related to the increasing  $\delta_L$ . The local asymmetry

parameter is seen when  $E_{sym}$  at (9 ~ 11) MeV which means that the emergence of  $\delta_L$  begins to occur in the region of neutron drops. Discontinuities are seen at  $E_{sym} \approx 22 \text{ MeV}$ , which means it indicates the

magnitude of the symmetry energy at the beginning of the paste phase. The increase  $E_{sym}$  which is stable enough to make  $\delta_L$  increase up to  $\rho \sim 2\rho_0$ .

Symmetry energy is very closely related to volume energy, this can be seen in the equation (13) and **Figure 8**.

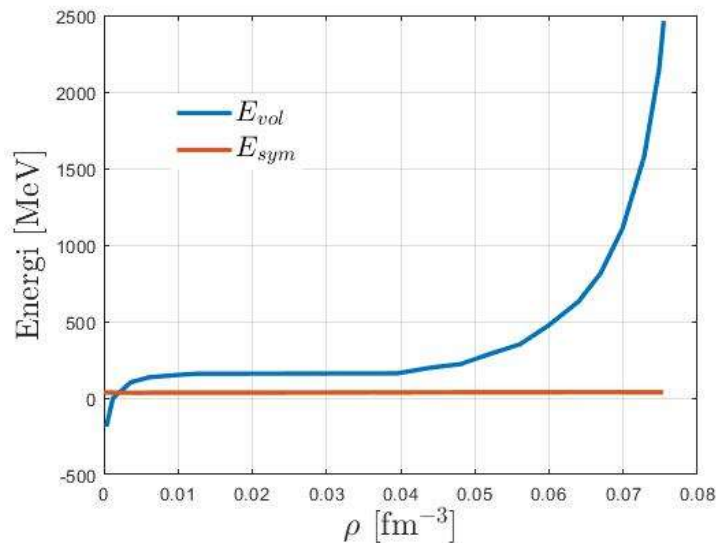


**Figure 8.** Energy change versus density

The relationship between the symmetry energy represented by the parameters  $J$  and  $L$  and volume energy can be seen in **Figure 8**. The parameter  $J$  itself is the volume symmetry energy as an approximation of the volume contribution to the liquid drop model (Paweł Danielewicz and Lee, 2009). In the neutron drop region, the symmetry energy makes the volume energy positive with a fairly gentle energy increase in the range of (20 ~ 145) MeV. However, the increase in symmetry energy as a function of density around (21 ~ 24) MeV near the paste phase, can make the volume energy increase very rapidly, this can occur because the atoms begin to be unable to maintain their shape so that the binding energy comparable to the volume energy is very dominating.

From the above research results, it can be said that symmetry energy has a major role in identifying each region in neutron stars through its relationship with density, proton fraction or asymmetry parameters. The increasing symmetry energy leads to a greater abundance of neutrons in each atomic nucleus and can give rise to absorbed neutrons, which can be indicated by the presence of the local asymmetry parameter. The rise in symmetry energy also causes a decrease in the proton fraction value from the beginning of the neutron drip region, and can significantly enhance the volume energy as it enters the neutron star pasta phase.

## CONCLUSIONS

From the above discussion, it can be concluded that the effect of symmetry energy on the inner crust of neutron stars is seen in the increase in symmetry energy along with an increase in the

density of neutron stars causing equilibrium  $\beta^-$  to occur and produces *neutron excess* which is represented by  $\delta L$ , so that the number of  $N$  at the interface regions of the outer crust and the inner crust was increased by a number of  $Z$  valuing between 40 to 50. The increase in the number of neutrons makes the proton fraction decrease significantly, which can be seen from the beginning of entering the inner crust (neutron drop region). The increase in symmetry energy also leads to an increase in binding energy represented by volume energy as the main energy contribution with parameters  $J$  and  $L$  as parts of the volume energy. Within this equation,  $J$  is the volume symmetry energy that serves as an approximation of the volume contribution to the liquid drop model.

## REFERENCES

- Baldo, M., & Burgio, G. F. (2016). The Nuclear Symmetry Energy. *Progress in Particle and Nuclear Physics*, *91*, 203–258. <https://doi.org/10.1016/j.pnpnp.2016.06.006>
- Baym, G., Bethe, H. A., & Pethick, C. J. (1971). Neutron Star Matter. *Nuclear Physics, Section A*, *175*(2), 225–271. [https://doi.org/10.1016/0375-9474\(71\)90281-8](https://doi.org/10.1016/0375-9474(71)90281-8)
- Baym, G., Pethick, C. J., & Sutherland, P. (1971). The Ground State of Matter at High Densities : Equation of State and Stellar Models. *The Astrophysical Journal*, *170*, 299–317.
- Chamel, N., & Haensel, P. (2008). Physics of

- Neutron Star Crusts. *Living Reviews in Relativity*, 11, 1–201. <https://doi.org/10.12942/lrr-2008-10>
- Danielewicz, P., & Lee, J. (2009). Symmetry Energy I: Semi-Infinite Matter. *Nuclear Physics A*, 818(1–2), 36–96. <https://doi.org/10.1016/j.nuclphysa.2008.11.007>
- Douchin, F., & Haensel, P. (2001). A Unified Equation of State of Dense Matter and Neutron Star Structure. *Astronomy and Astrophysics*, 380(A&A), 151–167. <https://doi.org/https://doi.org/10.1051/0004-6361:20011402>
- Fantina, A. F., Chamel, N., Mutafchieva, Y. D., Stoyanov, Z. K., Mihailov, L. M., & Pavlov, R. L. (2016). Role of The Symmetry Energy on The Neutron-Drip Transition in Accreting and Nonaccreting Neutron Stars. *Physical Review C*, 93(1), 1–12. <https://doi.org/10.1103/PhysRevC.93.015801>
- Gandolfi, S. (2013). The Equation of State of Neutron Star Matter and The Symmetry Energy. *Journal of Physics: Conference Series*, 420(1), 1–7. <https://doi.org/10.1088/1742-6596/420/1/012150>
- Grill, F., Providência, C., & Avancini, S. S. (2012). Neutron Star Inner Crust and Symmetry Energy. *Physical Review C - Nuclear Physics*, 85(5), 2–16. <https://doi.org/10.1103/PhysRevC.85.055808>
- Haensel, Paweł. (2001). Neutron Star Crusts. In *Physics of Neutron Star Interiors* (Vol. 578, pp. 127–174). [https://doi.org/10.1007/3-540-44578-1\\_5](https://doi.org/10.1007/3-540-44578-1_5)
- Haensel, P., Potekhin, A.Y., and Yakovlev, D.G. (2007). *Neutron Stars 1: Equation of State and Structure*, Astrophysics and Space Science Library, vol. 326, Springer, New York, U.S.A.
- Iida, K., & Oyamatsu, K. (2004). Surface Tension in A Compressible Liquid-Drop Model: Effects on Nuclear Density and Neutron Skin Thickness. *Physical Review C - Nuclear Physics*, 69(3), 1–4. <https://doi.org/10.1103/PhysRevC.69.037301>
- Istiqomah, E. L. (2010). *Suhu Kritis dan Celah Tenaga Superfluida pada Inti Bintang Neutron yang Mendingin* (Universitas Gadjah Mada). Retrieved from [http://etd.repository.ugm.ac.id/home/detail\\_pencarian/48767](http://etd.repository.ugm.ac.id/home/detail_pencarian/48767)
- Lattimer, J. M., & Prakash, M. (2004). The Physics of Neutron Stars. *Science*, 304(5670), 536–542. <https://doi.org/10.1126/science.1090720>
- Lattimer, James M., & Prakash, M. (2007). Neutron Star Observations: Prognosis for Equation of State Constraints. *Physics Reports*, 442(1–6), 109–165. <https://doi.org/10.1016/j.physrep.2007.02.003>
- Lee, C. H., Kuo, T. S., Li, G. Q., & Brown, G. E. (1998). Nuclear Symmetry Energy. *Physical Review C*, 57(6), 3488–3491. <https://doi.org/10.1103/PhysRev.109.117>
- Misner, C. W., Thorne, K. S., & Wheeler, J. A. (1973). *Gravitation*. San Francisco: Freeman & Company.
- Moustakidis, C. C. (2012). Symmetry Energy Effects on Location of The Inner Edge of Neutron Star Crusts. *Phys. Rev. C*, 1–12.
- Newton, W. G., Gearheart, M., Hooker, J., & Li, B. A. (2012). The Nuclear Symmetry Energy, The Inner Crust and Global Neutron Star Modeling. *Astrophysical Journal*, 1(1), 1–25.
- Oppenheimer, J. R., & Volkoff, G. M. (1939). On Massive Neutron Cores. *Physical Review*, 55(4), 374–381. <https://doi.org/10.1103/PhysRev.55.374>
- Oyamatsu, K., Iida, K., & Koura, H. (2010). Neutron Drip Line and The Equation of State of Nuclear Matter. *Physical Review C - Nuclear Physics*, 82(2), 2–5. <https://doi.org/10.1103/PhysRevC.82.027301>
- Pearson, J. M., Chamel, N., Fantina, A. F., & Goriely, S. (2014). Symmetry Energy: Nuclear Masses and Neutron Stars. *European Physical Journal A*, 50(2), 1–10. <https://doi.org/10.1140/epja/i2014-14043-8>
- Potekhin, A. Y. (2010). The Physics of Neutron Stars. *Physics-Uspekhi*, 53(12), 1235–1256. <https://doi.org/10.3367/ufne.0180.201012c.1279>
- Roca-Maza, X., & Piekarewicz, J. (2008). Impact of The Symmetry Energy on The Outer Crust of Nonaccreting Neutron Stars. *Physical Review C - Nuclear Physics*, 78(2), 1–11. <https://doi.org/10.1103/PhysRevC.78.025807>
- Sammarruca, F. (2014). Recent Advances in Microscopic Approaches to Nuclear Matter

- and Symmetry Energy. *Symmetry*, 6(4), 851–879. <https://doi.org/10.3390/sym6040851>
- Steiner, A. W., Prakash, M., Lattimer, J. M., & Ellis, P. J. (2005). Isospin asymmetry in nuclei and neutron stars. *Physics Reports*, 411(6), 325–375. <https://doi.org/10.1016/j.physrep.2005.02.004>
- Steiner, Andrew W. (2008). Neutron Star Inner Crust: Nuclear Physics Input. *Physical Review C - Nuclear Physics*, 77(3), 2–8. <https://doi.org/10.1103/PhysRevC.77.035805>
- Tolman, R. C. (1939). Static Solutions of Einstein's Field Equations for Spheres of Fluid. *Physical Review*, 55(4), 364–373. <https://doi.org/10.1103/PhysRev.55.364>
- Vidaña, I. (2020). Short Introduction to The Physics of Neutron Stars. *EPJ Web of Conferences*, 227, 1–8. <https://doi.org/10.1051/epjconf/202022701>
- 018
- Viñas, X., Gonzalez-Boquera, C., Sharma, B. K., & Centelles, M. (2017). Pasta-Phase Transitions in The Inner Crust of Neutron Stars. *Acta Physica Polonica B, Proceedings Supplement*, 10(1), 259–268. <https://doi.org/10.5506/APhysPolBSupp.10.259>
- Weber, F. (2005). Strange Quark Matter and Compact Stars. *Progress in Particle and Nuclear Physics*, 54(1), 193–288. <https://doi.org/10.1016/j.pnpnp.2004.07.001>
- Zhang, Z., & Chen, L. W. (2013). Constraining The Symmetry Energy at Subsaturation Densities using Isotope Binding Energy Difference and Neutron Skin Thickness. *Physics Letters, Section B: Nuclear, Elementary Particle and High-Energy Physics*, 726(1–3), 234–238. <https://doi.org/10.1016/j.physletb.2013.08.002>